Electronic Supplementary Material (ESI) for Inorganic Chemistry Frontiers.

Support Information

Table S1 The density(d) and the relative density(d_r) of BTS-xAg$_2$Se (x=0, 0.1, 0.15, 0.25 and 0.35 vol%).

BTS-$x$vol% Ag$_2$Se	d(g/cm^3)	d_r(%)
x=0	7.70	98.6%
x=0.10	7.58	97.1%
x=0.15	7.60	97.3%
x=0.25	7.50	96.0%
x=0.35	7.49	95.9%

where d_r is relative density, defined as $d_r=d/d_o$, here d is the measured density and d_o (7.81g/cm^3) is the theoretical density of $Bi_2Te_{2.5}Se_{0.5}$. For composite specimens $Bi_2Te_{2.5}Se_{0.5}$-$x$vol%Ag_2Se, the theoretical density is modified as: $d_o=(1-x)d_1 + xd_2$, where $d_1=d_o$ for BTS matrix and d_2 (8.05 g cm^{-3}) is the theoretical density of Ag_2Se.

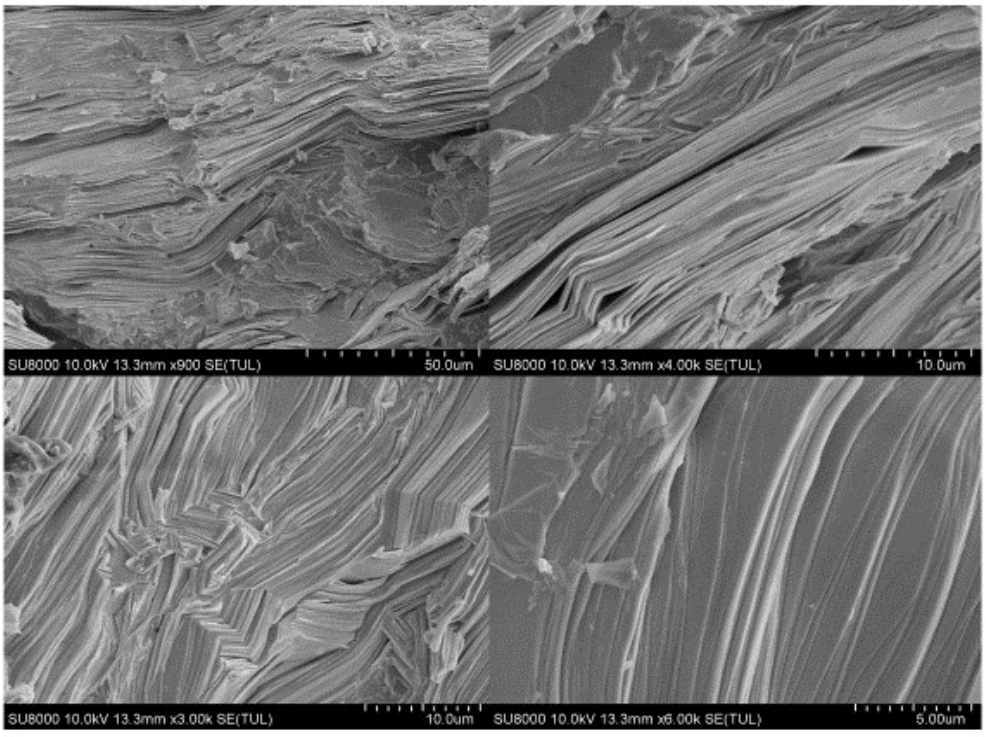

Fig. S1. SEM image of the fractured surface of the BTS.

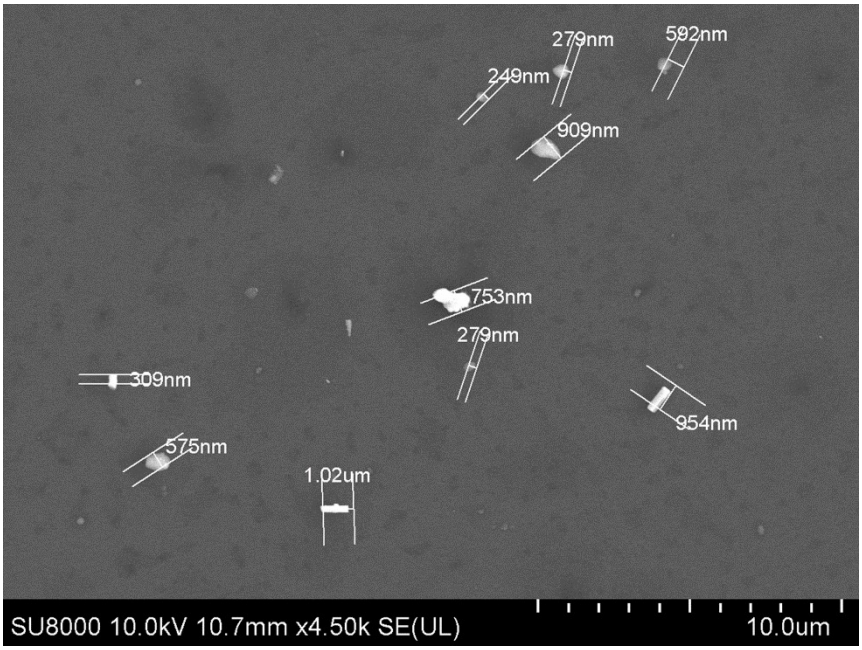

Fig. S2. SEM image of the Ag_2Se particle

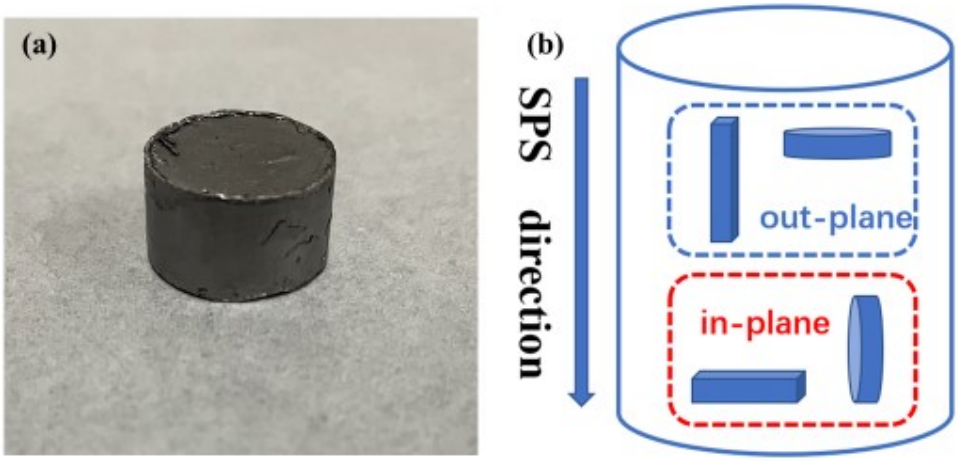

Fig. S3. Schematic illustration of the preparation of samples for measuring TE properties

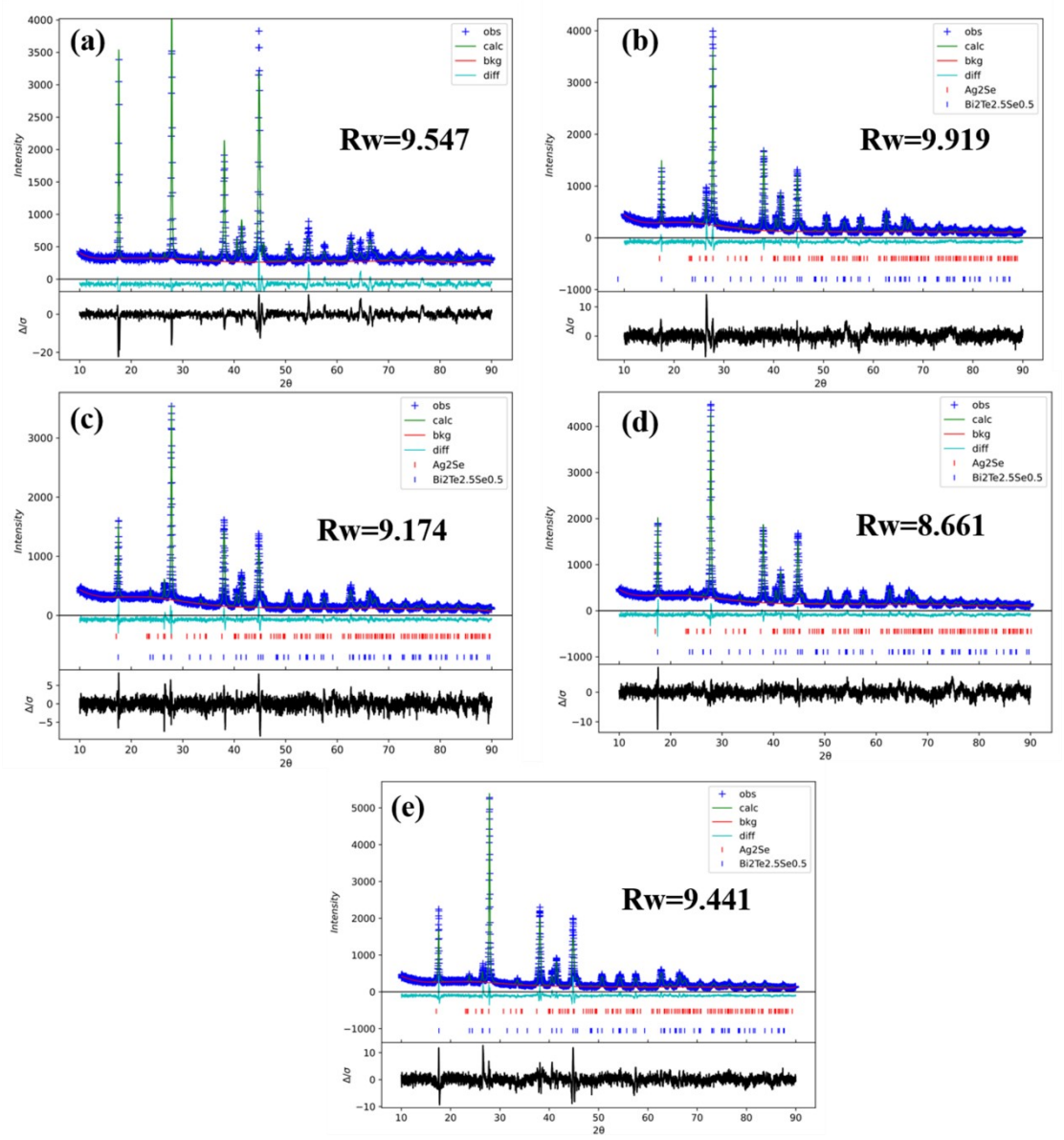

Fig. S4. The Rietveld refinement results for BTS-*x*Ag_2Se (*x*=0 (a), 0.10 (b), 0.15 (c), 0.25 (d) and 0.35 (e) vol%)

Calculation of L number

For metals or heavily doped degenerate semiconductors, *L* is constant and equals to $2.44\times10^{-8}W\Omega K^{-2}$, whereas it approaches $1.5\times10^{-8}W\Omega K^{-2}$ for nondegenerate semiconductors. On the basis of the single parabolic band (SPB) model with acoustic

phonon scattering dominating, the Lorenz number, L, can be derived from the following equations[1]:

$$L = \left(\frac{k_B}{e}\right)^2 \left(\frac{\left(\lambda + \frac{7}{2}\right) F_{r+\frac{3}{2}}(\eta)}{\left(\lambda + \frac{3}{2}\right) F_{r+\frac{1}{2}}(\eta)} - \left[\frac{\left(\lambda + \frac{5}{2}\right) F_{r+\frac{3}{2}}(\eta)}{\left(\lambda + \frac{3}{2}\right) F_{r+\frac{1}{2}}(\eta)} \right]^2 \right) \tag{S1}$$

$$F_n(\eta) = \int_0^\infty \frac{x^n}{1 + e^{x-\eta}} dx \tag{S2}$$

$$S = \pm \frac{k_B}{e} \left(\frac{\left(\lambda + \frac{5}{2}\right) F_{\lambda+\frac{3}{2}}(\eta)}{\left(\lambda + \frac{3}{2}\right) F_{\lambda+\frac{1}{2}}(\eta)} - \eta \right) \tag{S3}$$

where k_B is the Boltzmann constant, e is the electron charge, λ is the scattering parameter equaling to -0.5 for acoustic phonon scattering, $F_n(\eta)$ is the nth order Fermi integral and η is the reduced Fermi energy, which can be calculated from the measured Seebeck coefficient according to Equation S3. The results are shown in the Figure S5.

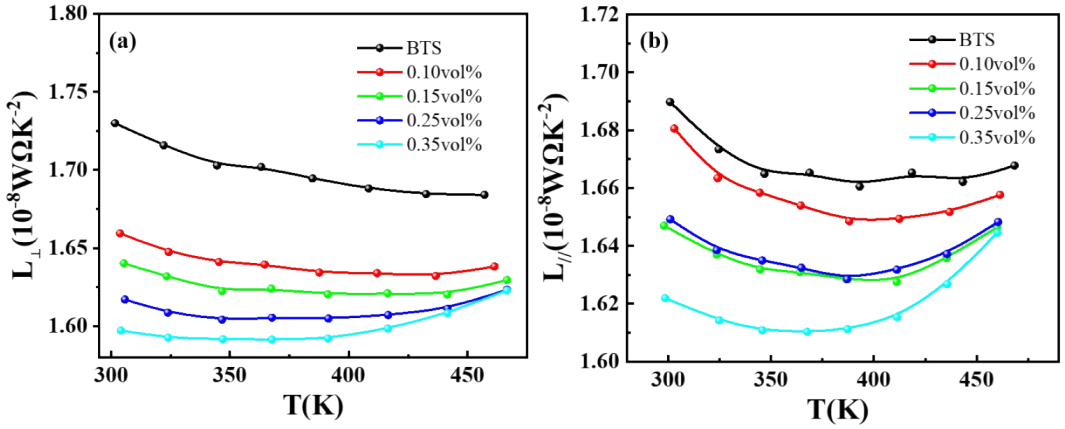

Fig. S5. The Lorentz number normal (a) and parallel (b) to the SPS direction for BTS-xAg$_2$Se (x=0, 0.1, 0.15, 0.25 and 0.35 vol%).

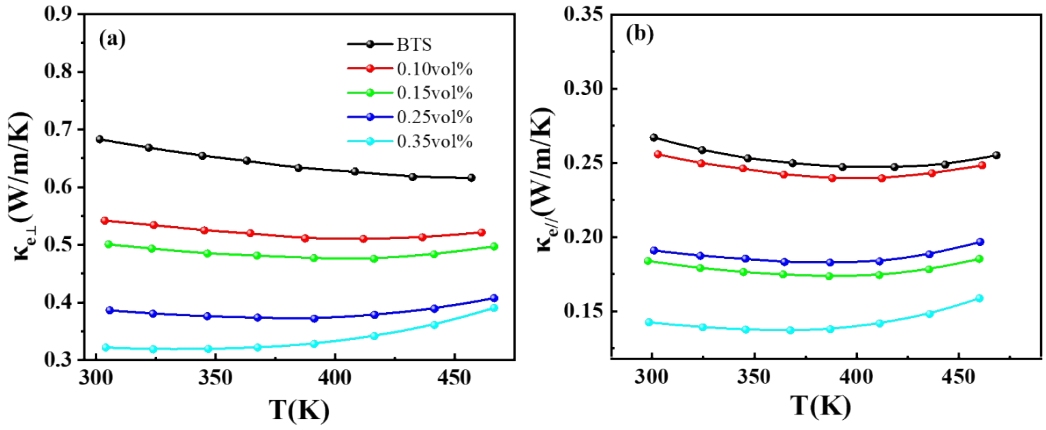

Fig. S6. The electron thermal conductivity normal (a, $\kappa_{e\perp}$) and parallel (b, $\kappa_{e//}$) to SPS direction for BTS-*x*Ag_2Se (*x*=0, 0.1, 0.15, 0.25 and 0.35 vol%).

Calculation of Lattice Thermal Conductivity

The lattice thermal conductivity κ_L can be calculated by using the Debye-Callaway model[2]:

$$\kappa_L = \frac{4\pi k_B^4 T^3}{\nu h^3} \int_0^{\frac{\theta}{T}} \tau(\varsigma) \frac{\varsigma^4 e^{\varsigma}}{(e^{\varsigma}-1)^2} d\varsigma \tag{S4}$$

where h, k_B, θ, ν, ς, and τ are the Planck constant, Boltzman constant, Debye temperature, phonon velocity, dimensionless variable, and total phonon relaxation time, respectively. τ is associated with the multiple scattering centers, which can be expressed as[3]

$$\frac{1}{\tau} = \frac{1}{\tau_U} + \frac{1}{\tau_N} + \frac{1}{\tau_{PD}} + \frac{1}{\tau_B} + \frac{1}{\tau_{NP}} + \frac{1}{\tau_{DS}} \tag{S5}$$

where τ_U, τ_N, τ_{PD}, τ_E, τ_B, τ_{NP} and τ_{DS} are relaxation time corresponding respectively to the scattering from phonon-phonon U- and N-process (U+N), point defects (PD), phase boundaries (B), and nanoparticles (NP), dislocation strain fields and dislocation cores (DS).

$$\tau_U^{-1} = \frac{\hbar \gamma^2 \omega^2 T}{M v^2 \theta_D} e^{-\theta_D/3T}$$

$$\tau_N^{-1} = \beta\tau_U^{-1} = \beta\frac{\hbar\gamma^2\omega^2 T}{M v^2 \theta_D} e^{-\theta_D/3T}$$

$$\tau_{PD}^{-1} = \frac{V\omega^4}{4\pi v^3}\Gamma$$

$$\tau_B^{-1} = v/l$$

$$\tau_{NP}^{-1} = v[(2\pi R)^2 + \left(\frac{4\pi R^2}{9}\left(\frac{\Delta D}{D}\right)^2\left(\frac{\omega R}{v}\right)^4\right)^{-1}]^{-1} N_P$$

$$\tau_{DS}^{-1} = 0.6 B_D^2 N_D \gamma^2 \omega\left\{\frac{1}{2} + \frac{1}{24}\left(\frac{1-2r}{1-r}\right)^2\left[1 + \sqrt{2}\left(\frac{v_L}{v_T}\right)\right]\right\} + N_D\frac{v^{-4/3}}{v_s^2}\omega^3$$

$$A = \frac{V\omega^4}{4\pi v^3}\Gamma$$

$$B = (1+\beta)\frac{\hbar\gamma^2\omega^2 T}{M v^2 \theta_D} e^{-\theta_D/3T}$$

$$C = 0.6 B_D^2 N_D \gamma^2\left\{\frac{1}{2} + \frac{1}{24}\left(\frac{1-2r}{1-r}\right)^2\left[1 + \sqrt{2}\left(\frac{v_L}{v_T}\right)\right]\right\}$$

$$D = N_D\frac{v^{-4/3}}{v_s^2}$$

In the case of our sample, the total scattering rate τ^{-1} can be shortened as

$$\frac{1}{\tau} = A\omega^4 + B\omega^2 \exp\left(-\frac{\theta_D}{3T}\right) + \frac{v}{l} + v\sigma N_p + C\omega + D\omega^3 \qquad \text{(S6)}$$

In the equation above, ω is the phonon frequency and *l* is the average spatial distance among the nanoinclusions Ag_2Se in BTS while v/*l* corresponds to scattering from the phase boundaries.

To quantitatively calculate κ_L, the literature values[4]of Debye temperature θ_D =164K and sound velocity ν=1778m s^{-1} are used for BTS-*x*Ag_2Se (*x*=0, 0.1, 0.15, 0.25 and

0.35 vol%). l is the average spatial distance between the Ag_2Se nanoparticles in the BTS, $\Delta D/D$ = 0.134 and the average radius of Ag_2Se (R) is 620nm; the pre-factors of point defect A, U- and N- process B, dislocation strain fields and dislocation cores C and D and the number density of nanoparticles N_P are provided in Table S2

Table S2. Parameters used in Debye-Callaway model for BTS-$x$$Ag_2Se$ samples (x=0, 0.1, 0.15, 0.25 and 0.35 vol%).

	0vol%	0.10vol%	0.15vol%	0.25vol%	0.35vol%
$A(10^{-42}S^3)$	5.45	5.45	5.45	5.45	5.45
$B(10^{-17}Sk^{-1})$	3.23	3.23	3.23	3.23	3.23
C	0	0.006	0.006	0.006	0.006
$D(10^{-30}s^2)$	0	2.8	2.8	2.8	2.8
l	--	599	599	671	711
$N_p(10^{17}m^{-3})$	--	2.9	3	0.91	0.67

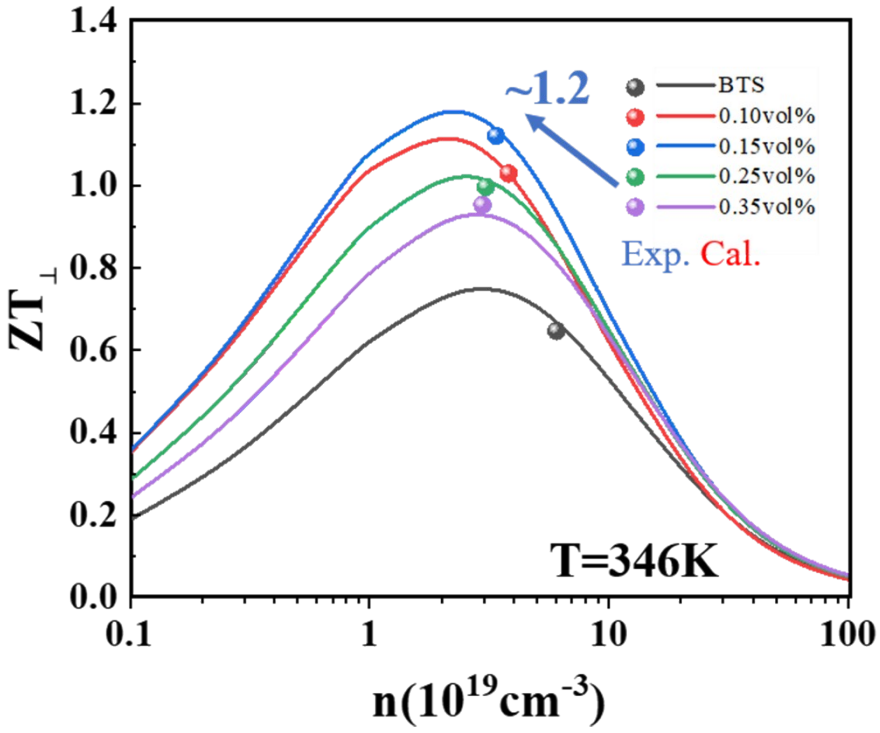

Fig. S7. Calculated $ZT_{\perp}$ as a function of n by a SPB model, the experimental ZT values are provided for comparison.

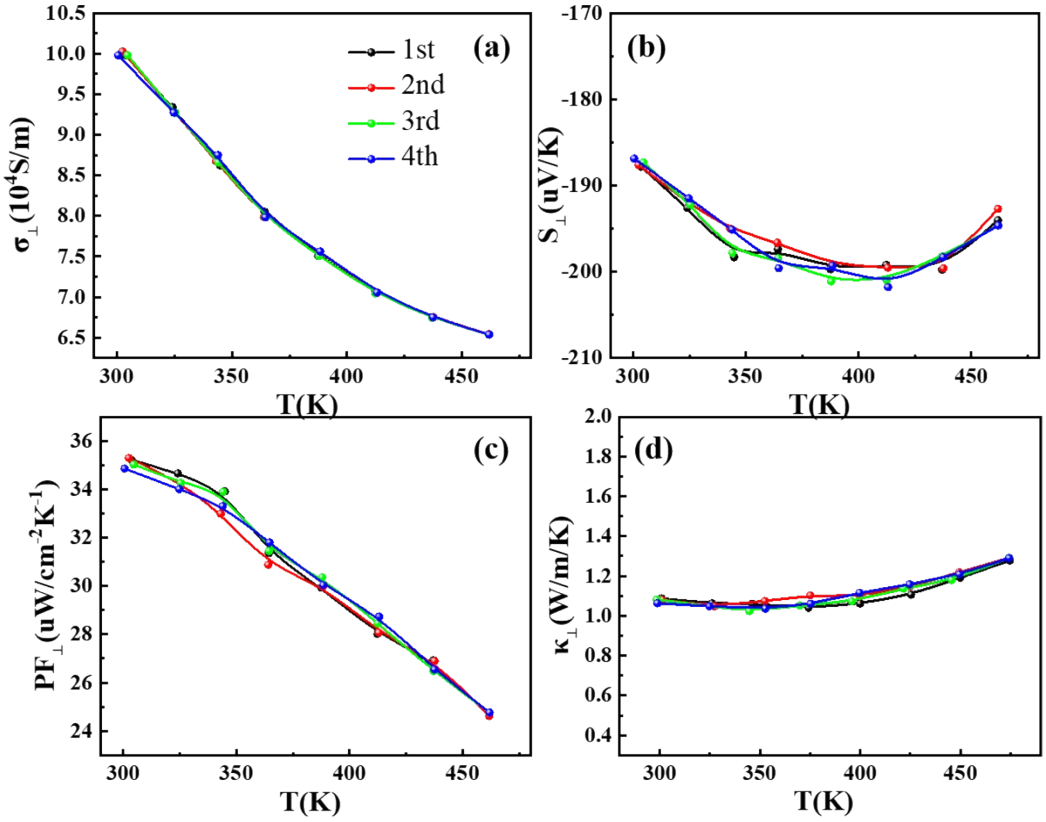

Fig. S8. Data repeatability of electrical conductivity (a), Seebeck coefficient (b), power factor (c) and thermal conductivity (d) normal to the SPS direction for BTS-0.15vol%Ag_2Se sample

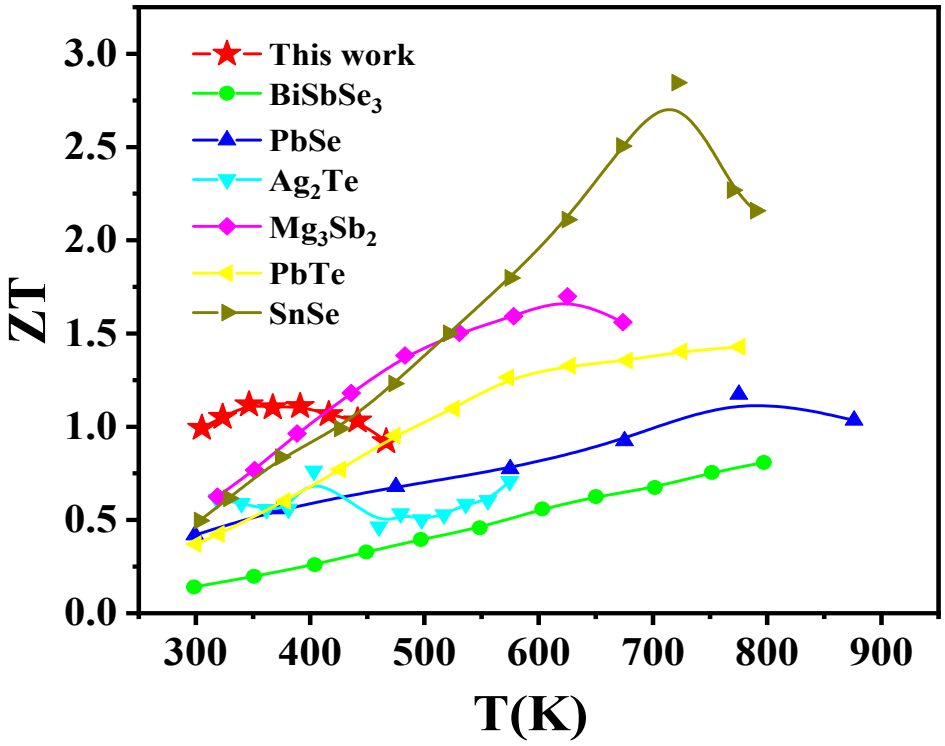

Fig. S9. The temperature dependence of ZT for some typical N-type thermoelectric materials[5-10].

From the Fig.S9，we can see the BTS-0.15vol%Ag_2Se material has superior low-temperature thermoelectric performance in the low temperature region, which is better than other n-type systems.

Reference

1. Zhu B, Liu X, Wang Q, et al. Realizing record high performance in n-type Bi_2Te_3-based thermoelectric materials. Energy & Environmental Science, 2020, 13(7): 2106-2114.

2. J. Callaway, H.C. von Baeyer, Physical Review, 120 (1960) 1149-1154

3. Ming H, Zhu C, Chen T, et al. Creating high-dense stacking faults and endo-grown nanoneedles to enhance phonon scattering and improve thermoelectric performance of Cu_2SnSe_3. Nano Energy, 2022, 100: 107510.

4. Chen T, Ming H, Qin X, et al. Enhancing the thermoelectric performance of n-type $Bi_2Te_{2.7}Se_{0.3}$ through the incorporation of Ag_9AlSe_6 inclusions. Inorganic Chemistry Frontiers, 2022, 9(20): 5386-5393.

5. Shi H N, Y, Qin Y.X, B.C. Qin B.C, et al. Incompletely Decomposed In_4SnSe_4 Leads to High-Ranged Thermoelectric Performance in n-Type PbTe, Adv. Energy Mater.

6. Su L Z, Wang D Y, Wang S N, et al. High thermoelectric performance realized through manipulating layered phonon-electron decoupling, Science 375 (2022) 1385.

7. Wang S N, Wang D Y, Su L Z, Y. et al. Realizing synergistic optimization of

thermoelectric properties in n-type $BiSbSe_3$ polycrystals via co-doping zirconium and halogen, Mater. Today Phys. 22 (2022) 7.
8. Xiao Y , Xu L Q , Hong T, et al. Ultrahigh carrier mobility contributes to remarkably enhanced thermoelectric performance in n-type PbSe, Energy Environ. Sci. 15 (2022) 346-355.
9. Hu H, Xia K, Wang Y, et al. Fast synthesis and improved electrical stability in n-type Ag_2Te thermoelectric materials. Journal of Materials Science & Technology, 2021, 91: 241-250.
10. Zhang F, Chen C, Yao H, et al. High-performance N-type Mg_3Sb_2 towards thermoelectric application near room temperature. Advanced Functional Materials, 2020, 30(5): 1906143.